Simulation and implementation of heat load shifting in a low carbon dwelling

*John Allison [1], Andrew Cowie [1], Stuart Galloway [2], John Hand [1], Nick Kelly [1] *, Bruce Stephen [2]*

[1] Energy Systems Research Unit, University of Strathclyde, Glasgow, G1 1XJ, UK
[2] Institute for Energy and Environment, University of Strathclyde, Glasgow, G1 1XW, UK
* Corresponding author. Email: nick@esru.strath.ac.uk; Tel. +44 (0)141 574 5083; Fax +44 (0)141 552 5105

Abstract
A predictive load shifting control system for a heat pump has been developed and installed in a low carbon test house located at the BRE Innovation Park, Motherwell, near Glasgow. The house features an exhaust-air source heat pump supplying an under floor heating system. The controller predicted the day-ahead space heating requirements for the house, based on forecast air temperatures and solar radiation levels and then automatically set the heat pump's start and stop times for the following day. The heat pump's operation was restricted where possible to off-peak electricity tariff periods (00:00-07:00). The controller's operating parameters were pre-set using a calibrated building simulation model. After installation, the controller's performance was monitored during September 2015 and analysis of test data showed that the predictive control maintained indoor air temperatures between 18-23^{o}C for around 87% of notional occupied hours between 07:00-22:00; this was better than predicted by simulation. However, the energy performance of the heat pump was extremely poor as it did not function well under intermittent load-shifting operation, with the majority of the heat was delivered primarily by an auxiliary immersion coil rather than the heat pump itself. The paper concludes with suggestions for refinements to the controller and further work.

Keywords: heat pump; load shifting; field trial; building simulation; predictive control.

Nomenclature

C	Next day's space heating charge (kWh)
H	Heating system capacity (kW)
S_o	Solar insolation (W/m^2)
T_e	External air temperature (^{o}C)
t_s	Heating start time (hour.hour fraction)

1 Introduction

The domestic sector faces a range of challenges as the UK attempts to drastically cut its carbon emissions by 2050. Key issues are reducing the overall demand for heat and decarbonising the residual heat loads, which encompass both space heating and hot water provision. If the supply of electricity in the UK is progressively decarbonised at the macro and micro-scales through the deployment of renewable generation, then the electrification of heat using heat pumps would be an effective means to provide the low-carbon space heat, hot water (and possibly cooling) required by the domestic sector. However, the widespread adoption of heat pumps would significantly increase the power flows on the electricity network. Wilson et al. [1] indicated that a shift of only 30% of domestic heating to heat pumps could result in an increase of 25% in the total UK electrical demand. To mitigate the potential negative impacts of heat pumps, particularly on peak demand and reduce or delay network upgrade costs, load shifting of household thermal demands may become essential.

There have been many papers published, focusing on load shifting of household heat demands and their impacts. Callaway [2] modelled the potential for manipulation of large populations thermostatically controlled loads to follow variable renewable generation. Wang et al [3] modelled the potential for load shedding in a large population of many thousands of unbuffered domestic heat pumps by manipulating of the space heating set point.

At the level of the individual dwelling, Hong et al. [4, 5] simulated heat pump load shifting and found that shifts in heat pump operating times of up to 6-hours were possible in thermally improved dwellings, but only with the addition of up to 500L of hot water thermal buffering. Again using a model, Arteconi et al [6] investigated the use of buffering in less well-insulated buildings, indicating that up to 800L of buffering would be required to deliver only 1-hour of load shifting. Kelly et al [7] modelled load shifting of heat pump demand to off-peak periods in low carbon housing and found that to avoid discomfort, up to 1000 L of hot water thermal buffering would be required.

The majority of papers reviewed in the literature on load shifting are based on modelling studies and there is little work focusing on the application of domestic heat load shifting to real buildings and the impact of load shifting on indoor conditions and systems operation. To address this issue, this paper describes the development of a load shifting control system for a domestic heat pump, its installation in a real building and an analysis of thermal performance under load shifting control. The novel features of the work reported are 1) the use of a calibrated simulation model to pre-define the parameters for a load shift controller; 2) the implementation of a cloud-based, load shift heat pump controller and its application to a real building; and 3) the monitoring of the energy and environmental performance of load shifting over several weeks. The load shifting was assessed from an indoor environmental performance perspective – so the thermal conditions achieved in the test building are a key metric for the success or failure of the load shifting approach.

2 Method

The load shift field trial described here involved six stages of activity. These were as follows.

1. Deployment of monitoring equipment and acquisition of performance data;
2. development and calibration of a simulation model of the test house;
3. use of the model to identify the parameters for a predictive control algorithm;
4. assessing the virtual effectiveness of load shifting using simulation;
5. implementation of the load shift controller in the real test house; and
6. monitoring and assessment of actual performance under load shifting.

2.1 The test house and initial monitoring

The building used for the tests – the Applegreen House - is located at BRE Ltd's Innovation Park, Motherwell near Glasgow (55.78° N, 3.99° W). It is intended to be a demonstration of a mass-market, low-cost, modular-build, low-carbon house. The building is shown in Figure 1. The house is steel framed, has a slab-on-grade concrete foundation with a flat-roof construction. The roof is weatherproofed using bituminous felt. The building is clad in insulated panels, which are externally rendered; the upper half of the building also features external timber cladding. Windows are double-glazed. The interior of the house is finished with plaster-on-stud and carpeted throughout.

Figure 1: The Applegreen house at the BRE Innovation Park, Motherwell.

The house has a total floor area of 127m^2 spread over an upper and lower floor and has an internal volume of 304m^3. As the house is a test facility, it was unoccupied during the reported experiments; the implications of this are discussed later in the paper. Heating and hot water are provided by a 3/5kW NIBE F470 air source heat pump – the heat delivered to the house is recovered from the exhaust air. The maximum heat pump output is 3kW; a 5kW direct electric immersion coil is also available if required.

Note that, initial measurements of the heat pump system installed in the test house indicated that almost all of the heat was supplied by the 5kW immersion coil due to a low return temperature from the floor preventing the compressor from operating; this was caused by the heat pump being operated intermittently for the tests described in this paper. As load shifting specifically requires intermittent operation of the heat pump, the work proceeded on the assumption that the heat supplied from the heat pump would be the 5kW from immersion heater output; this assumption was later confirmed in the analysis of the monitored results.

The heat pump was coupled in to a mechanical ventilation system with the evaporator located in the extract duct, acting as a heat recovery system. The mechanical ventilation system delivered 55 L/s of outside air or approximately 0.65 ACH. Unlike the tank-buffered heat pump systems, which feature heavily in the literature (e.g. Arteconi et al. [6]; Hong et al. [4]), the Applegreen House heat pump here serves an under floor heating system, which supplies the lower and upper floors. The heat is delivered into pipes embedded into the floor screed, which is approximately 70mm deep. The floor mass therefore acts as storage and a thermal buffer between the heat pump and the house. The heat pump includes an internal 170 L hot water tank. A system schematic is shown in Figure 2. However hot water demand was not considered in these tests.

The house also features a 3 kW PV array on the rooftop which feeds into the house supply after power conditioning and inversion.

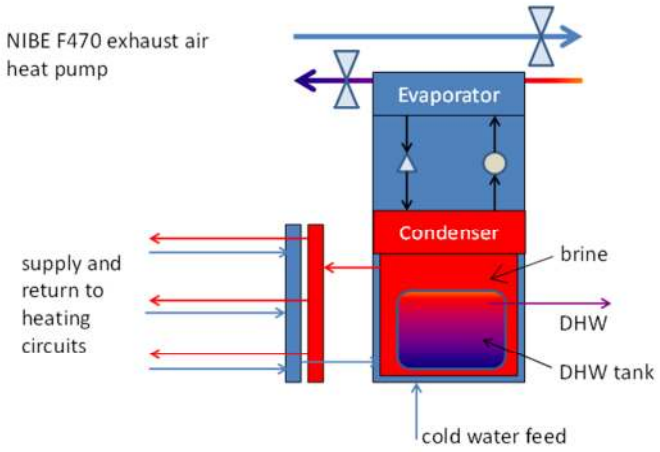

Figure 2: Schematic of air source heat pump and ventilation system.

Prior to developing a model, the key thermal characteristics of the house were established from the building plans and using a blower door test. Additionally, the temperature of the house and climate data was monitored for several months prior to the experiment commencing for additional calibration data. The blower door results indicated that the fabric leakage rate was 3 air-changes-per-hour when pressurised to 50 Pa. Under normal operating conditions this translates to leakage rate of 0.06 air-changes-per-hour.

The data acquisition system used a wireless Eltek RX250AL Receiver/Logger along with three Eltek wireless transmitters; two of these were used to measure indoor temperature and relative humidity, and the final transmitter was used to measure the current at the consumer unit. During the monitored period, total electrical amperage was recorded; this was converted into watts, assuming a voltage of 230 V.

A laptop running a customised data acquisition algorithm polled the logger for monitored data and uploaded this via a web service interface to a UK-based cloud server at 10 min intervals. Each upload held two sets of 5 min data readings from the transmitters.

The instrumentation also included a rooftop weather station supplied by Campbell Scientific, which measured direct and diffuse solar radiation, external air temperature and RH, wind speed and direction. Readings were recorded at 5 minute intervals. This data was downloaded manually and merged with the data from the logger. An example of the collected data is shown in Figure 3, which shows the variation in indoor temperatures and external conditions.

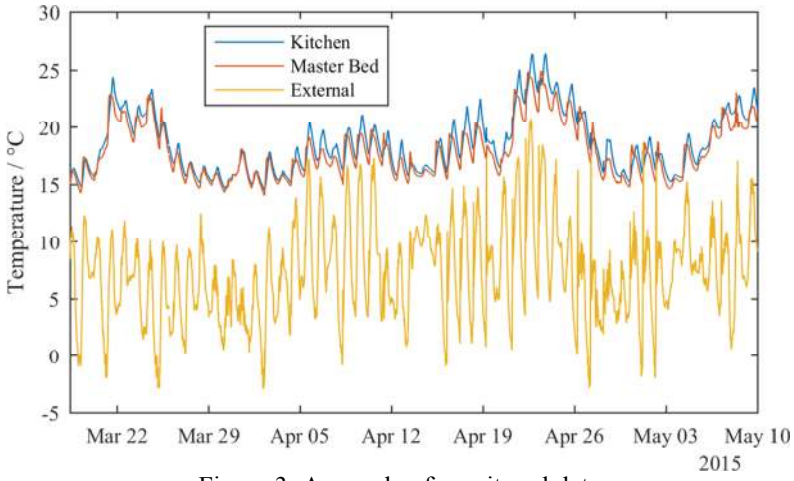

Figure 3: A sample of monitored data

2.2 Simulation model and calibration

A model of the test house was developed using the ESP-r building simulation tool [8]. An ESP-r model is a thermodynamic representation of a building, which typically comprises three core constituents.

1. The 3-D geometry of the building is divided into thermal zones, a zone being a notionally enclosed volume within the building, typically corresponding to a specific room. The zone volume is bounded by surrounding surfaces, such as an external wall, internal wall, window, floor, etc. The enclosed space can be modelled at different resolutions: typically the space is modelled as a well-mixed volume at a homogeneous temperature, with heat transfer coefficients used to account for phenomena such as stratification; alternatively the volume can be replaced by a CFD 'domain' [8]. The latter approach has been adopted in this case as this has been demonstrated to provide

sufficient accuracy for systems and controls modelling [9]. However, if the function of the analysis was ventilation analysis then the CFD approach would be more appropriate.

2. Materials data - each surface has one or more layers that correspond the material layers seen in the real building, with each layer comprising a specific material type. ESP-r uses a large materials database, which holds information on the following material properties for a wide range of common building materials: conductivity k, density ρ, specific heat c_p, absorptivity and emissivity (-). Additional data is held for transparent materials relating to solar transmission τ, reflection γ and absorption α, at different angles of incidence (0, 40, 55, 70, 90^o).
3. The geometric and materials data is augmented with schedules that define the magnitude and time variation of internal heat gains from occupants and equipment along with user defined heating control set points, which can be used in the calculation of the time varying heat demand for the building.

The resolution of the core model was also improved with the addition of an airflow network model. This is used to define bulk airflow paths [10] to determine the bulk buoyancy and pressure driven air flow between zones along with pressure and buoyancy driven infiltration and influence of mechanical ventilation. The model geometry along with a schematic of the airflow network is shown in Figure 4.

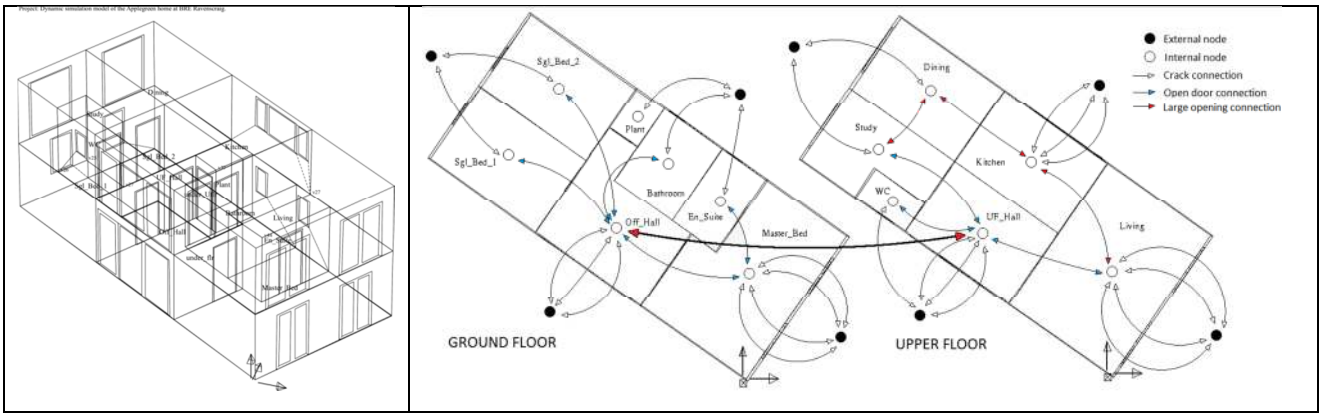

Figure 4: Images of the 3-D geometry of the building model and corresponding air flow network model.

The mathematical basis of ESP-r has been described exhaustively elsewhere in more detail by Clarke [8], so only a summary is provided here. In the tool, a building model (zones, surfaces, networks) is decomposed into thousands of control volumes a control volume being an arbitrary region of space to which conservation equations for energy (thermal and electrical), continuity, momentum, species can be applied and one or more characteristic equations formed. The number of equations depends on the resolution of the model. In this case, only the energy and continuity equations are required for each control volume. A typical model of a building will contain thousands of such volumes, with sets of equations extracted and grouped according to the physical system (e.g. transfer, fluid flow, power flow, etc.). The equations that describe the heat transfer associated with the building fabric are linearised and solved directly, using a mixed implicit-explicit formulation that is unconditionally stable. The bulk fluid flow and power flow equations (if required) are solved iteratively, and converge for the vast majority of cases. The ESP-r tool and its solution method have been the subject of extensive validation activities over many years; these are described by Strachan et al. [9]. The solution of these equations sets with real time series climate data, coupled with control and occupancy-related boundary conditions yields the dynamic evolution of temperature, energy and fluid flows within the building and its supporting systems.

The house model is available for examination and use, and can be download from: http://fits-lcd.org.uk/file_uploads/Other/173158__Applegreen_Calibrate.tar.gz. ESP-r is available from: https://github.com/ESP-rCommunity/ESP-rSource. A summary of the geometric and fabric details of the model is provided in Tables 1a and b.

Table 1a: Summary details of Applegreen house model thermal zones.

Zone name	Level	Volume m^3	Glazing m^2	Façade m^2	Partitions/ ceiling/floor m^2	Floor m^2
Master bedroom	Ground	44.9	3.24	26.4	52.4	18.7
Office & entry	Ground	28.3	9.6	3.6	48.1	11.8
Bedroom 1	Ground	25.4	0.9	15.1	37.1	10.6
Bedroom 2	Ground	25.4	0.9	15.1	37.1	10.6
Plant room	Ground	3.6	0	2.5	12.4	1.5
Bathroom	Ground	13.9	0.3	4.8	29.6	5.8
En-Suite	Ground	10.6	0.3	3.6	25.6	4.4
Living	Upper	50.8	11.2	48.4	27.5	21.2

Upper hall	Upper	25.2	9.5	14.2	29.0	10.5
WC	Upper	5	0.3	6.3	11.8	2.1
Study	Upper	20.5	12.4	17	19.5	8.5
Dining	Upper	25.4	18.9	23.6	10.6	10.6
Kitchen	Upper	25.2	14.9	17.9	19.8	10.5

Table 1b Summary details of Applegreen house model internal and external constructions.

Description	Thickness (mm)	Number of layers	Mass per m^2	U-value (W/m^2K)	Area in building (m^2)
Ground level Façade wall	235	7	72.3	0.2	67
Upper level Façade wall	242	5	67.6	0.2	58.8
Thick acoustic partition	165	7	47.5	0.306	55.9
Thin non-acoustic partition	90	3	40.9	1.38	14.1
Thin acoustic partition	95	5	35.0	0.53	74.3
Internal door	50	1	29.2	1.8	29.5
Glazing frame	69	2	44.6	1.46	9.9
Façade glazing	26	3	25	1.21	30.2
Roof (flat)	271	6	109	0.18	63.3
Ground level floor	530	4	677	0.18	63.3
Intermediate floor	435	5	352	0.4	59.6

The model's predictions of indoor air temperature were calibrated using the weather and indoor temperature data collected in the months leading up to the setting-up of the load shifting experiment. This calibration was a multi-stage process that involved 1) iteratively manipulating the characteristics air flow network flow connections to the exterior of the building, shown in Figure 4, until a match was achieved between average infiltration and the value from the blower door test. 2) Next, the monitored heat input (assumed to be equivalent to the measured background electrical demand) was imposed on the model as a heat gain profile; the air flow network connections between the indoor nodes were modified to achieve temperature difference between the two floors broadly commensurate with the monitored data. 3) Finally, building fabric U-values were degraded to account for thermal bridging and other building defects. The wall U-values emerging from this process are as shown in Table 1b. The air temperature predictions of the model against measured data are shown in Figure 5. The model typically produces air temperatures within ±1 °C of measured conditions and the model accurately follows the trends in temperature fluctuations seen in the measured data. The accuracy of the sensors is ±0.1 °C. For the purposes of controller development, this level of accuracy was deemed sufficient.

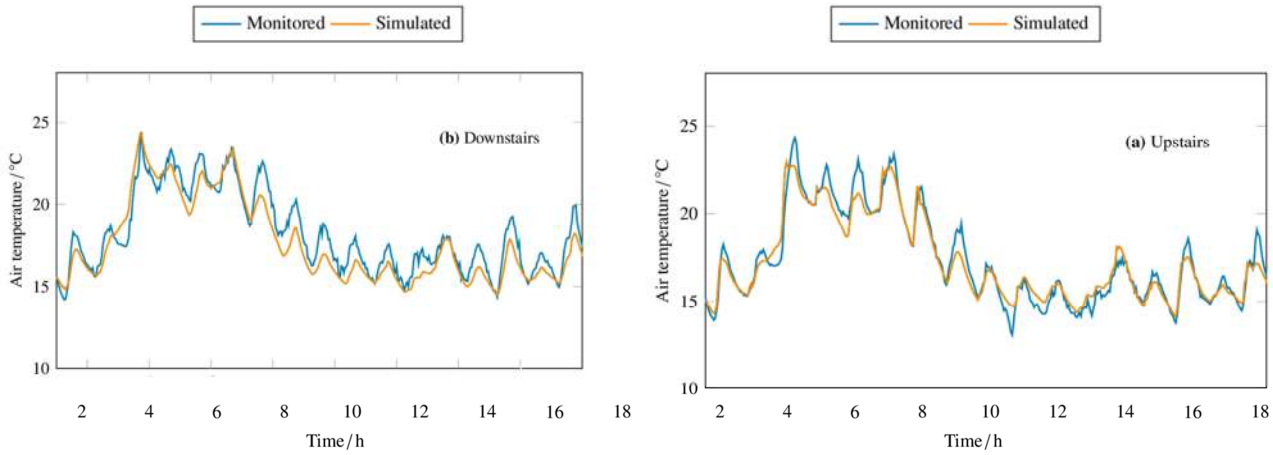

Figure 4: Monitored and predicted indoor temperatures.

As the test house used an under floor heating system, the most accurate measure of thermal comfort would be the dry resultant temperature (DRT); which comprises both the mean radiant temperature and the air temperature. However, the monitoring equipment installed in the test house could only measure the air temperature. The simulation data was analysed to assess the impact of this shortcoming and its potential implications for comfort assessments.
Table 2 shows an analysis of the difference between the air and DRT for the test house with the under floor heating system active.

Table 2: Difference between simulated air and dry resultant temperatures.

	Min / °C	Max / °C	Mean / °C
Zone dry bulb T	11.3	35.7	21.2
Mean Radiant T	15.4	38.4	22.0
Zone Resultant T	13.9	36.0	21.6
|dry bulb T – Resultant T|	2.6	0.3	0.4

At the minimum house temperature, there was an appreciable difference of over 2°C between the air and DRT. However, low temperatures such as this tended to occur outside periods of active occupancy and the difference at higher temperatures and the overall average difference was less than 1°C, indicating that for the majority of time, the difference between the two temperatures was small. Based on these findings, it was assumed that the air temperature alone could act as a reasonable proxy for comfort conditions.

2.3 Identifying controller parameters

The simulation model was used to identify the parameters for the heat pump load shift controller – charge and operating time. Firstly, to determine the charge required to heat the house to comfort conditions over a range of climatic conditions an annual simulation was run. Secondly, a series of simulations were run to determine if the calculated heat load could successfully be delivered during off peak periods whilst still maintaining indoor comfort conditions.

The annual simulation used a Glasgow climate dataset (the closest available to the house's location). A heating control algorithm was employed, which maintained the indoor air temperatures between 18 and 23°C between the hours of 07:00-22:00 hrs. The resulting heat demands from the simulation were then used along with the climate data to develop a polynomial heating equation that estimated the next day's heating charge required as a function of the next day's average temperature (°C) and average solar insolation (W/m^2); this is as follows.

$$C = 77.84 - 2.545T_e - 0.3745S_o - 0.06873{T_e}^2 - 0.002453T_eS_o + 0.001232{S_o}^2 + 0.0005543{T_e}^2S_o - 4.789 \times 10^{-6}T_e{S_o}^2 - 1.517 \times 10^{-6}{S_o}^3 \quad (1)$$

This equation was used later as a day-ahead heat charge predictor for the load shift controller.
Note that the equation as shown does not include an allowance for internal occupant gains as the house was not occupied during the tests. However, a similar expression for heating charge, accounting for gains could be developed by including a suitable occupancy pattern in the simulation model.
Equation 1 was derived from a surface fitted to the simulated daily heating charge (marked points in Figure 5).

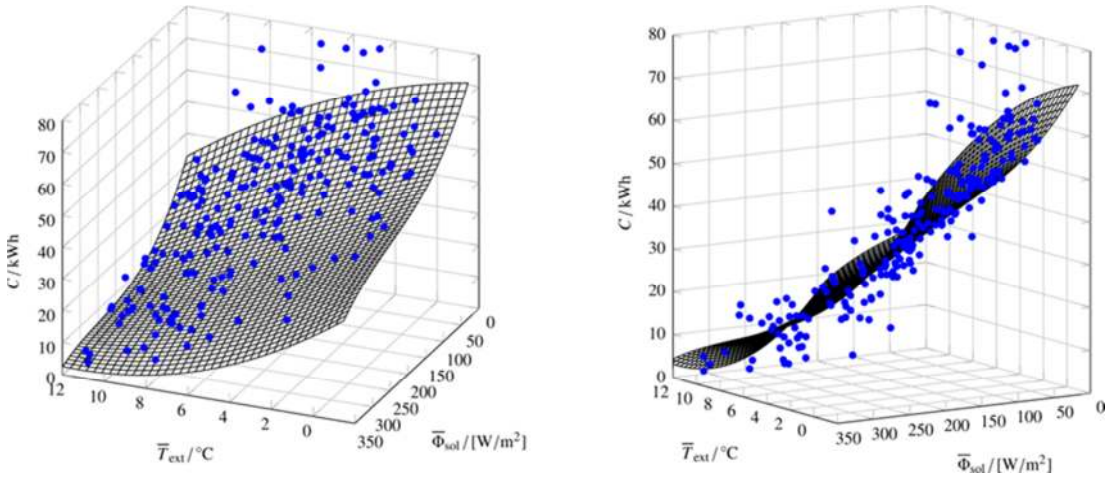

Figure 5: Plot of surface fitted to simulated daily heating charge.

2.4 Testing controller using simulation

The impact of shifting the heating charge to off-peak periods (00:00-07:00) was initially investigated using the model. The simulations used a modified version of the ESP-r tool, which featured the day-ahead heating charge equation as part of a new controller; this calculated the next-day heating charge using the following day's temperature and solar

data from the model's climate file (Glasgow climate data set). The algorithm then calculated a day-ahead off-peak heating start time based on the following equation.

$$t_s = 7 - \frac{C}{H}; \frac{C}{H} \leq 7$$
$$t_s = 24 + \left(7 - \frac{C}{H}\right); \frac{C}{H} > 7 \quad (2)$$

Here, t_s is the start time (decimal hours) and H is the heating system capacity (in this case 5 kW).
Note that where the calculated charge and 5kW capacity resulted in a charge time of greater than 7 hours, the charge would begin the evening of the day before. The charge was delivered into the under floor screed of the model's lower and upper floor constructions.
Assessment of the load shifting looked at the temperatures achieved in the house between 0700-2200. If temperatures fell below 18°C or rose above 23°C, then the load shift would be deemed infeasible as this would result in some discomfort for the building occupants. However, the results from the load shift simulations indicated that the heating load could be moved to off peak periods without serious discomfort occurring, with temperatures remaining between 18-23°C for approximately 84% of notional occupied hours. This was due to two main factors. Firstly, the house fabric was well insulated, which limited temperature drops during unheated periods. Secondly, the upper and lower floor screed acted as a substantial thermal store – approximately 8.61m^3 of screed material. Together, the insulated fabric and floor thermal capacity allowed the house to ride through the unheated period of 07:00-22:00 without temperatures dropping significantly.

2.5 Controller implementation

Once it was established that off-peak load shifting was feasible and would not seriously affect comfort, a remote load shifting control system was developed for the house. This comprised the following elements.

1) heat pump control interface;
2) monitoring and data acquisition system; and
3) load shift controller.

The NIBE heat pump used in the house could be accessed remotely using an internet interface or SMS-based interface. The SMS-based interface was chosen for this work as, unlike the internet interface, the heat pump data could be accessed by 3rd party applications. The SMS interface allowed the heat pump to be switched on and off and also allowed the heat pump internal data to be accessed if required.
The heat pump controller (based around Equation 1) and supporting software operated within a Linux-based cloud server and carried out the following tasks.

- The controller parsed a day-ahead weather forecast from a meteorological web service and used it to calculate the average air temperature and total solar insolation for the following day; this was done at hourly intervals over the preceding day to capture changes in the forecast. The control algorithm used the forecast data to calculate the heating charge and associated heating charge time and start/stop times for the heat pump.
- At the calculated times, the on/off control signals were passed to the heat pump in the test house using the Twilio SMS web API which allows cloud based applications to send and receive voice calls and SMS messages.

The communications and data logging system are illustrated in Figure 6.

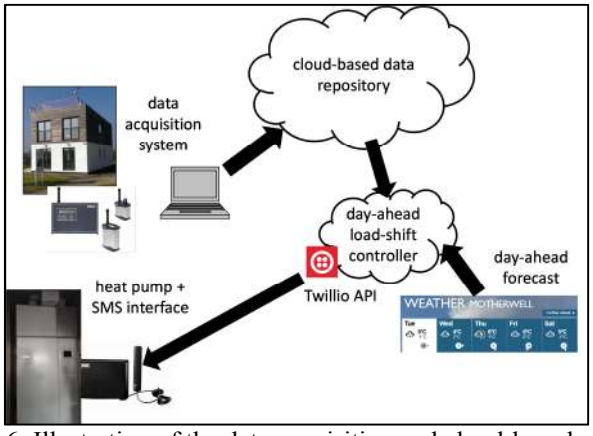

Figure 6: Illustration of the data acquisition and cloud-based control.

2.6 Testing and monitoring

The performance of the controller was tested during September 2015, a period when daytime temperatures had dropped enough for the heat pump to run for appreciable periods of time.
The field trials comprised two elements.

1. The control system was tested under manual operation – a forecast of the following days weather was obtained and Equations 1 and 2 was used to determine the heating start time; this was passed to the heat pump using an SMS message sent from the IF mobile phone application: IF allows tasks to be logic controlled and time scheduled. The purpose of these manual tests was simply to test viability of the approach.
2. The heat pump was then subject to fully automated control using the cloud based controller, this calculated the heating charge and subsequent start/stop times and passed these directly to the controller. The output from the controller and monitored data was streamed to a live website.

3 Results

Analysis of the indoor air temperatures indicated that they remained between 18 and 23°C for 87% of the time between 07:00 and 22:00, when the heat pump was operated under load shifting control (Figure 7). The remaining 13% of the monitored period, temperatures were above 23°C but less than 25°C.

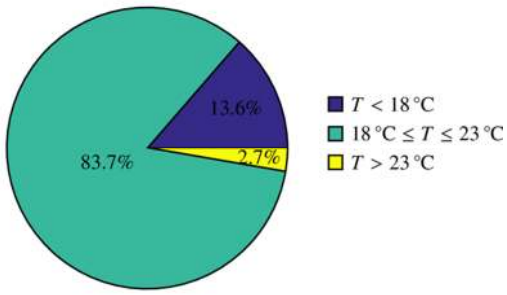

Figure 7: The breakdown of indoor temperatures over the September test period.

As the heat was pre-delivered into the floor screed, the heating system tested was unable to respond to disturbances after the initial charging period. So, for example, greater than forecast levels of solar radiation would lead to higher indoor air temperatures than predicted.
Figure 8 shows typical conditions from the test from Sept 8 – Sept 12. Higher temperatures occurred when solar gains pushed indoor temperatures above 23°C. Note that on the two days with the highest solar radiation the calculated charge was zero. On the 4th day in Figure 8, solar gains push the upper floor air temperature marginally above 23°C.

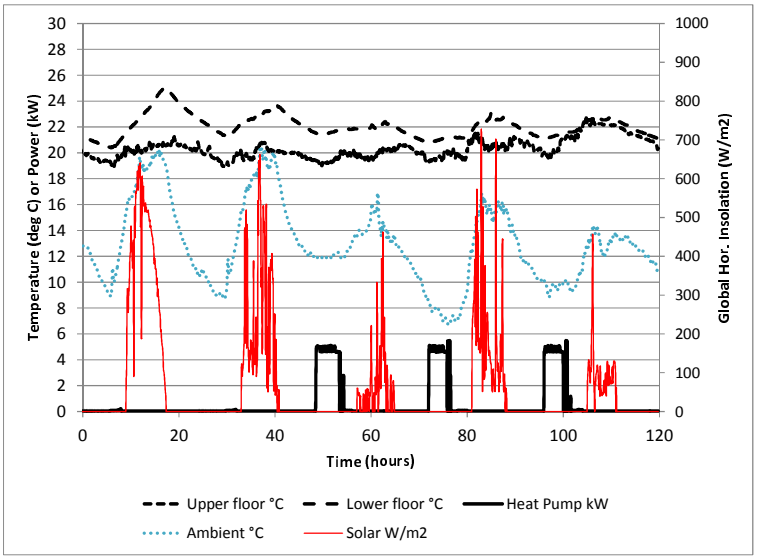

Figure 8: Measured heat pump charge and indoor temperatures Sept 8 – Sept 12.

The total energy consumption of the heat pump during September was 434 kWh and the total run time was 91 hrs. This gives an average power consumption of 4.8 kW and indicates (as was suggested by the initial tests) that the heat supply was almost all from the auxiliary heating coil rather than the heat pump itself. This is evident in the power demand plot in Figure 8.

4 Discussion and conclusions

A full scale demonstrator for thermal load shifting in a low carbon house has been established at BRE's Innovation Park near Glasgow. The house features an exhaust air heat pump and under floor heating.

The house thermal characteristics were tested and a calibrated building simulation model developed, this was used to identify the parameters for a load shift controller – the day-ahead heat charge and the charge start/stop times.

A remote load-shift control system was established which included in-house environmental monitoring and a cloud-based data logging.

The controller used an algorithm derived from the building simulation model coupled with a day-ahead weather forecast to set the following day's operating time for the heat pump.

The full load shifting system was tested during September 2015 with results from the tests indicating that load shifting of the full space heating charge to off-peak-periods (00:00-07:00) was feasible for the test house without any substantial under or overhearing occurring during nominal occupied periods.

Temperatures in occupied periods generally remained between 18 and 23^{o}C. Peak temperatures were below 25^{o}C. Significant solar gains occasionally pushed the upper floor temperature above 23^{o}C; as the heating charge had already been delivered to the floor slab, the system was unable to respond to this disturbance.

As the building was unoccupied during the tests, the impact of occupation was not accounted for – this would include heat gains from occupants and disturbances due to opening and closing external doors and windows. However, the same combination of modelling and testing could be used to develop new controller parameters and verify the efficacy of control in an occupied dwelling.

Finally, the energy performance of the house's exhaust air heat pump proved to be extremely poor. Analysis of the current drawn by the unit showed that the demand during off peak heating periods was approximately 5kW; this indicated that almost all of the heat was supplied to the house was by the unit's auxiliary immersion heater with a coefficient of performance (COP) of 1.0, rather than the heat pump itself, which has a nominal COP of 3.0. Subsequent investigation revealed that the compressor rarely switched on due to a low exhaust air temperature alarm; something that is unavoidable with intermittent off-peak operation. It is unclear whether this problem is intrinsic to the design of the heat pump, or whether the control settings of the unit were poorly set during commissioning.

5 Further work

There are a number of areas where the work reported here could be further developed. These are as follows.

The house was unoccupied during the test, so the impact of heat gains from occupants and occupant activity on the performance of the load-shifting algorithm could not be assessed; further research would require tests on an occupied house or at least include simulated occupancy.

The heating system tested here included under floor heating, which supports extensive time shifting of the thermal load. However, such under floor heating is really only an option for load shifting in new housing. Experiments with the heat pump buffered using a storage tank would provide valuable insight into the performance and limits of load shifting when retrofitted into older house types.

The heat pump system control was limited to on and off. Future heat pump systems will feature compressors that can be modulated; allowing more nuanced manipulation of heat pump output to be implemented.

The predictive heating equation can be further refined by including the current day's indoor temperature.

The exhaust air heat pump used in these trials was unable to operate effectively with intermittent operation. A more conventional air source heat pump system using outside air would be recommended for future trials.

Finally, the work reported here focused on space heating. In an occupied house the provision of hot water heating would also need to be accommodated by the load shift controller.

6 Acknowledgements

The work reported here was primarily funded under the Grand Challenge Research Programme – Top and Tail of Energy Networks. The authors gratefully acknowledge the finding received from Engineering and Physical Science Research Council (EPSRC) under grant EP/I031707/1 and for the help given to them by other members of the consortium. The work also utilised technology developed under EPSRC grants EP/L024489/1 - Pervasive sensing for collaborative facilities management and EP/N021479/1 – Fabric integrated thermal storage in low carbon dwellings. The authors would like to acknowledge the generous help that they received from BRE Ltd. and Applegreen Homes Ltd. in making the test house available for the experiments reported in this paper. The authors are also grateful for access to climate data provided by Dr Paul Baker of Glasgow Caledonian University.

7 References

1. Wilson I A G, Rennie A J R, Ding Y, Eames P C, Hall P J & Kelly N. 'Historical daily gas and electrical energy flows through Great Britain's transmission networks and the decarbonisation of domestic heat' Energy Policy; 61; 2013; pp301-305.
2. Callaway D. Tapping the energy storage potential in electric loads to deliver load following and regulation, with application to wind energy. Eng. Convers. and Management; v50;(9); 2009; pp. 1389-1400.

3. Wang D, Parkinson S, Miao W, Jia H, Crawford C, Djilali N. Online voltage security assessment considering comfort-constrained demand response control of distributed heat pump systems, Appl. Energy. 96; 2012; pp104–114.
4. Hong J, Kelly N J, Thomson M, Richardson I. The influence of thermal storage on microgeneration flexibility. Proc. the 2nd Int. Conf. in Microgeneration Technologies. University of Strathclyde, Glasgow; 2011; pp1-8.
5. Hong J, Kelly N J, Thomson M, Richardson I. Assessing heat pumps as flexible load. Proc. of the IMECHE Part A: J of Power and Eng. v227(1); 2013; pp30-42.
6. Arteconi A, Hewitt N J , Polonara F. Domestic demand-side management (DSM): Role of heat pumps and thermal energy storage (TES) systems. Appl. Therm. Engineering. 51; 2013; pp155-165.
7. Kelly N J, Tuohy P G, & Hawkes A D. Performance assessment of tariff-based air source heat pump load shifting in a UK detached dwelling featuring phase change-enhanced buffering. Applied Thermal Engineering, 71(2); 2014; pp809-820.
8. Clarke J A. Energy Simulation in Building Design. 2nd Ed. Butterworth-Heinemann: Oxford; 2001.
9. Strachan P, Kokogiannakis G, & Macdonald I. History and development of validation with the ESP-r simulation program. Building and Environment, 43(4); 2008; pp601-609.
10. Hensen J L M. 'On the thermal interaction of building structure and heating and ventilating systems', PhD Thesis, Eindhoven University of Technology, 1991.